Sensors & Transducers, Vol. 153, Issue 6, June 2013, pp. 129-140

www.sensorsportal.com

Sensors & Transducers

http://www.sensorsportal.com

Model to Analyze Micro Circular Plate Subjected to Electrostatic Force

Cao Tian-Jie

The Airport College, Civil Aviation University of China, Tianjin 300300, China

Tel.: 86-22-24092476, fax: 86-22-24092470

E-mail: caotianjie@sohu.com

Received: 26 April 2013 /Accepted: 14 June 2013 /Published: 25 June 2013

Abstract: In this paper a distributed model with three possible static modes was presented to investigate the behavior of the plate subjected to electrostatic force and uniform hydrostatic pressure both before pull in and beyond pull in. The differential governing equation of the micro circular plate specifically used for numerical solution of the three modes, in which the singularity at the center of the micro plate did not occur, was presented based on the classical thin plate theory, Taylor's series expansion and Saint-Venant's principle. The numerical solution to the differential governing equation for the different mode was mainly attributed to solve for one unknown boundary condition and the applied voltage, which could be obtained by using a two-fold method of bisection based on the shooting method. The voltage ranges over which the three modes could exist and the points where transitions occurred between the modes were computed. Incorporating the above numerical solution to the applied voltage at the normal mode with some constrained optimization method, pull-in voltage and the corresponding pull-in position can automatically be obtained. In examples, the entire mechanical behavior of the circular plate over the operational voltage ranges was investigated and the effects of different parameters on pull-in voltage were studied. The obtained results were compared with the existing results and good agreement has been achieved. *Copyright © 2013 IFSA.*

Keywords: Micro circular plate, Pull-in voltage, Electrostatic force, Uniform hydrostatic pressure, Numerical solution.

1. Introduction

Electrostatically deflected elastic systems are studied in microelectromechanical systems (MEMS), such as microswitches and micropumps because of low power consumption, fast response time and high efficiency. All such systems exhibit a static instability phenomenon which is known as the pull-in instability, and in the design of such systems the static instability or pull-in phenomenon is of great practical importance. The static instability analysis of these systems started in the late 1960s by Nathanson et al. [1] (it was Nathanson who introduced the name pull-in instability) and Taylor [2]. Since their pioneering work, numerous investigators have analyzed and developed mathematical models of electrostatic actuation, such as lumped element models [3-5], one-dimensional distributed models [6-9], and three-dimensional finite element models [10-11] in attempts to understand further and control the static instability. Simple lumped element models of MEMS actuators with a single degree of freedom result in easy calculations but fail to capture details of the behavior, such as the bending moment and the shearing force. Three-dimensional finite element models lead to a detailed and accurate prediction, but simulations are expensive in time and computation, particularly for problems involving mechanical

contacts such as those in microswitches. One-dimensional distributed models can give useful results with reasonable effort, and the results are in well agreement with those obtained with three-dimensional finite element models. Micro circular plates are used in many microelectromechanical devices as micropump [12, 13], micro pressure sensors [14], microphones [15] and micro resonators [16]. Soleymani et al. [12] used a distributed model to investigate the pull-in instability of a circular plate subjected to nonlinear distributed electrostatic force with a finite difference method. Nabian et al. [13] also used the distributed model to investigate the pull-in instability of a circular plate subjected to nonlinear non-uniform electrostatic pressure and uniform hydrostatic pressure, in which in order to linearize the non-linear governing equation, a step by step linearization method was used and then the linear system of equation was solved by finite difference method. Liao et al. [17] obtained closed-form solutions for both the position and the voltage of the static pull-in event by considering the first-order deflection mode and using a fifth-order Taylor's series expansion of the electrostatic force.

In this paper a distributed model with three possible static modes (normal mode, transition mode and touch mode) will be used to investigate both the pull-in instability and beyond the pull-in instability of a circular plate subjected to non-uniform electrostatic pressure and uniform hydrostatic pressure. The entire mechanical behavior of a micro circular plate under both non-uniform electrostatic pressure and uniform hydrostatic pressure is modeled accordance with a thin Kirchhoff plate theory. Three possible static modes of the plate along with an intermediate dielectric layer between electrodes are first introduced. The non-linear differential governing equation is then modified for numerical solution of the first two modes by means of Taylor's series expansion and Saint-Venant's principle. The modified differential governing equation is without singularity at the center of the plate, and so it can be used for numerical solution. Last the modified differential governing equations for the three different modes are solved by a numerical method. In the method the solution to the modified differential governing equation is mainly attributed to solve for one unknown boundary condition and the applied voltage, which can be obtained by using a two-fold method of bisection based on the shooting method. In addition, some constrained optimization method, in which the objective is the pull-in voltage ,the variable is the deflection at the center of the plate, and the constraint is that the deflection at the center of the plate is between 0 and some largest value, may be used to obtain the pull-in voltage and the corresponding pull-in position. That is, solution to the pull-in voltage is to find a value of the deflection at the center of the circular plate at the normal mode that maximizes the applied voltage. In examples, the entire mechanical behavior of the circular plate over the operational voltage ranges is investigated and the effects of different parameters, such as radius and thickness of the plate, thickness of the dielectric layer, uniform hydrostatic pressure, uniform residual stress and initial gap on the pull-in voltage are studied.

2. Three Modes

As Fig. 1 shows, an electrostatic micro actuator [12, 13] with a pair of parallel circular plates is considered, and the model for mechanics analysis is shown in Fig. 2, in which g is the initial gap between the circular plate and the dielectric layer, t is the thickness of the circular plate, U is the applied voltage between the circular plate and the substrate, q_0 is the hydrostatic pressure, t_1 is the thickness of the dielectric layer, a is the radius of the circular plate, and w is the deflection of the circular plate at radius r.

The micro circular plate illustrated in Fig. 2 has three possible modes [18, 19] over the operational voltage range. These modes differ in the boundary conditions at the center of the circular micro plate and are as follows.

(i) Normal mode. The region before the top plate reaches the dielectric layer above the substrate is referred as the normal mode operation. At the mode, the micro circular plate has no contact with the dielectric layer and is illustrated in Fig. 3(a). The first derivative of w with respect to r or angle of rotation and the shearing force at the center of the plate are both equal to zero because of symmetry.

(ii) Transition mode. The plate touching the dielectric layer only at the center is said to be the transition mode operation. At the mode, only the center of the micro circular plate touches the dielectric layer and is illustrated in Fig. 3 (b). At the beginning of the transition mode, that is at the end of the normal mode, the second derivative of w with respect to r reaches a minimum(an absolute maximum), and at the end of the transition mode, i.e. the beginning of the touch mode, the second derivative of w with respect to r at the center has become to zero.

(iii) Touch mode. When a part of the micro circular plate is in contact with the dielectric layer, the electrostatic micro actuator works in touch mode, as illustrated in Fig. 3(c), and the contact radius of the micro circular plate Δ varies with the applied voltage. The first and the second derivatives of w with respect to r are both equal to zero at the points separating the contact and the non-contact regions of the micro circular plate.

The first two modes represent boundary value problems while the third mode represents a free boundary problem [6].

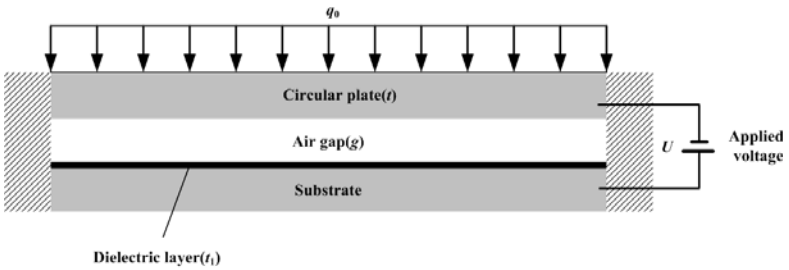

Fig. 1. Schematic diagram of an electrostatic.

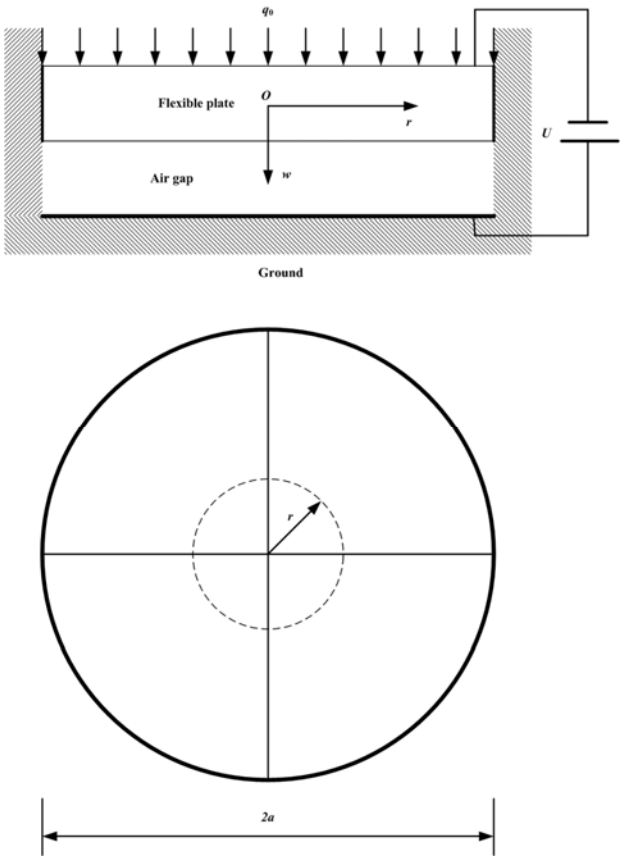

Fig. 2. The model for mechanics analysis.

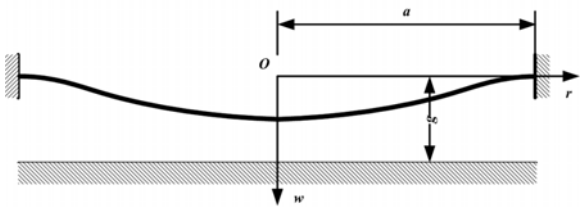

Fig.3 (a). Normal mode operation.

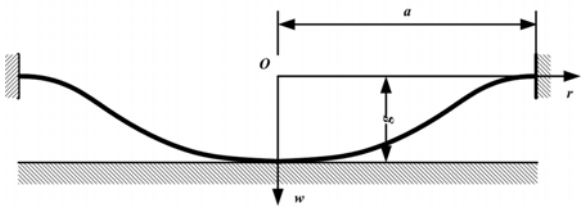

Fig. 3 (b). Transition mode operation.

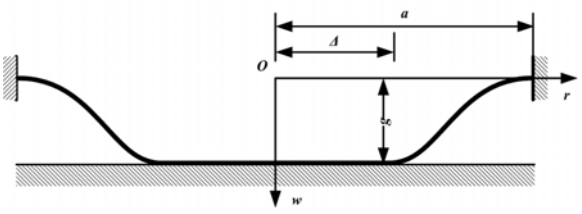

Fig. 3 (c). Touch mode operation.

3. Modification of Differential Governing Equation

The differential governing equations and the related boundary conditions differ at different modes. They are stated respectively as follows.

3.1. The Differential Governing Equation at the Normal Mode

The Kirchhoff (classical thin) circular plate theory with a uniform residual biaxial plane stress considered can be shown in general by following differential equation [13, 17]

$$D\left(\frac{d^4w}{dr^4}+\frac{2}{r}\frac{d^3w}{dr^3}-\frac{1}{r^2}\frac{d^2w}{dr^2}+\frac{1}{r^3}\frac{dw}{dr}\right)- \\ -\frac{\pi}{r}\frac{d}{dr}\left(r\frac{dw}{dr}\right)=q(r,w,U,q_0) \qquad 0\le r\le a \tag{1}$$

where $w(r)$ is the deflection of the plate a distance r form the center of the micro circular plate; τ is the uniform residual biaxial plane stress; $q(r)$ is the sum of both electrostatic and uniform hydrostatic pressure q_0; and D is the flexural rigidity which can be expressed as

$$D=\frac{Et^3}{12(1-\mu^2)}, \tag{2}$$

where E is Young's modulus; and μ is Poisson's ratio. The hydrostatic-electrostatic pressure applied a distance r form the center of the micro plate can be written as

$$q(r,w,U,q_0)=\frac{\varepsilon_0\varepsilon_r U^2}{2(G-w(r))^2}+q_0, \tag{3}$$

where U is the applied voltage; ε_0 is the vacuum permittivity; ε_r is the relative permittivity of air; G is the equivalent initial gap which can be written as

$$G=g+t_1/\varepsilon_1, \tag{4}$$

where ε_1 is the relative permittivity of the dielectric layer.

It can be seen from equation (1) that the singularity appears at the center $r=0$. As a result of the singularity at the center, equation (1) cannot be directly used for a numerical solution to a solid circular plate.

From Taylor's series expansion of r and under conditions the angle of rotation and the shearing force are both zero at the center by symmetry, one has

$$\begin{aligned}\frac{dw}{dr}&=\frac{d^2w(0)}{dr^2}r+\frac{1}{2}\frac{d^3w(0)}{dr^3}r^2+\frac{1}{6}\frac{d^4w(0)}{dr^4}r^3+O\left(r^4\right)\\ \frac{d^2w}{dr^2}&=\frac{d^2w(0)}{dr^2}+\frac{d^3w(0)}{dr^3}r+\frac{1}{2}\frac{d^4w(0)}{dr^4}r^2+O\left(r^3\right)\\ \frac{d^3w}{dr^3}&=\frac{d^3w(0)}{dr^3}+\frac{d^4w(0)}{dr^4}r+O\left(r^2\right)\end{aligned}, \tag{5}$$

where $O(\cdot)$ is "big oh" notation.

Substituting the above three expressions in equation (5) into the shearing force $Q(r)$ at the center, one has

$$\begin{aligned}Q(0)&=-D\lim_{r\to 0}\left(\frac{d^3w}{dr^3}+\frac{1}{r}\frac{d^2w}{dr^2}-\frac{1}{r^2}\frac{dw}{dr}\right)=\\ &=-1.5D\frac{d^3w(0)}{dr^3}=0\end{aligned} \tag{6}$$

Therefore, the differential equation (1) can be modified as

$$\begin{cases}D\left(\frac{d^4w}{dr^4}+\frac{2}{r}\frac{d^3w}{dr^3}-\frac{1}{r^2}\frac{d^2w}{dr^2}+\frac{1}{r^3}\frac{dw}{dr}\right)-\\ -\frac{\pi}{r}\frac{d}{dr}\left(r\frac{dw}{dr}\right)=q(r,w,U,q_0) \qquad 0<r\le a\\ D\frac{d^4w}{dr^4}=\frac{3}{8}q(0,w,U,q_0)+\frac{3\pi}{4}\frac{d^2w(0)}{dr^2}\\ \qquad\qquad\qquad\qquad\qquad\qquad r=0\end{cases} \tag{8}$$

The boundary conditions are

$$\frac{dw(0)}{dr}=\frac{d^3w(0)}{dr^3}=w(a)=\frac{dw(a)}{dr}=0 \tag{9}$$

Equation (8), which is the fundamentals in the numerical investigation of deflection for a micro circular plate in the paper, can now be used for a numerical solution because of no singularity at $r=0$.

3.2. The Differential Governing Equation at the Transition Mode

Because a concentrated reaction acts at the center of the circular plate at the transition mode, the moment and the shearing force at the center of the circular plate are all singular [20], and therefore equation (8) cannot be solved by a numerical method. By using Saint-Venant's principle [21], the concentrated force acted at the center of the circular plate can be replaced by a force distributed over a small circular area (in fact a concentrated force is a simplification for a force distributed over a small region), which is statically equivalent to the

concentrated force, in order for the singularity to vanish. Such a replacement of the concentrated force for a distributed force makes it possible for one to find the numerical solution to the problem.

As a result of using Saint-Venant's principle, the differential equation (8) can be further modified as

$$\begin{cases} D\left(\frac{d^4w}{dr^4}+\frac{2}{r}\frac{d^3w}{dr^3}-\frac{1}{r^2}\frac{d^2w}{dr^2}+\frac{1}{r^3}\frac{dw}{dr}\right)-\frac{\pi}{r}\frac{d}{dr}\left(r\frac{dw}{dr}\right)= \\ =q(r,w,U,q_0) \qquad \delta<r\le a \\ D\left(\frac{d^4w}{dr^4}+\frac{2}{r}\frac{d^3w}{dr^3}-\frac{1}{r^2}\frac{d^2w}{dr^2}+\frac{1}{r^3}\frac{dw}{dr}\right)-\frac{\pi}{r}\frac{d}{dr}\left(r\frac{dw}{dr}\right)= \\ =q(r,w,U,q_0)-q_1(r) \qquad 0<r\le\delta \\ D\frac{d^4w}{dr^4}=\frac{3}{8}q(0,g,U,q_0)-\frac{3}{8}q_1(0)+\frac{3\pi}{4}\frac{d^2w(0)}{dr^2} \\ r=0 \end{cases} \tag{10}$$

where δ is the radius of a small circular area; $q_1(r)$ is a force distributed over the area of radius δ.

The boundary conditions are

$$w(0)=g,\frac{dw(0)}{dr}=\frac{d^3w(0)}{dr^3}=w(a)=\frac{dw(a)}{dx}=0 \tag{11}$$

3.3. The Differential Governing Equation at the Touch Mode

At the touch mode, the differential governing equation without singularity is

$$\begin{cases} w(x)=g,\frac{dw(x)}{dr}=\frac{d^2w(x)}{dr^2}=0 \\ \qquad\qquad\qquad\qquad 0\le x\le\Delta \\ D\left(\frac{d^4w}{dr^4}+\frac{2}{r}\frac{d^3w}{dr^3}-\frac{1}{r^2}\frac{d^2w}{dr^2}+\frac{1}{r^3}\frac{dw}{dr}\right)-\frac{\pi}{r}\frac{d}{dr}\left(r\frac{dw}{dr}\right)= \\ =q(r,w,U,q_0) \qquad \Delta\le r\le a \end{cases} \tag{12}$$

The boundary conditions for the touch mode can be written as

$$w(\Delta)=g,\frac{dw(\Delta)}{dr}=\frac{d^2w(\Delta)}{dr^2}=w(a)=\frac{dw(a)}{dr}=0 \tag{13}$$

As soon as a non-zero Δ is given, equation (12) can be solved numerically under the above boundary conditions much more easily than the first two modes.

Touch mode capacitive pressure sensor has several advantages over normal mode sensor, such as good linearity, large operating pressure range, large overload protection and zero suppression possibility [22].

4. Numerical Solutions

In generally, if the applied voltage, the uniform hydrostatic pressure and four boundary conditions, the deflection and its first three derivatives, at the center of the circular micro plate are known, the deflection and the first three derivatives at any point then can easily be obtained numerically from the differential governing equations (8), (10) or (12) by using some numerical technique such as the adaptive Runge-Kutta-Fehlberg algorithm [23] which can automatically adjust the step size and stop the calculations when a certain prescribed error criterion, such as 10^{-6}, is met. Due to the three different configurations and therefore different boundary conditions, the unknowns at the center or at $r=\Delta$ of the micro circular plate are also different. The procedure of the numerical solution to equations (8), (10) or (12) for the three modes is stated respectively as follows. In the procedure, it is assumed that the uniform hydrostatic pressure is a constant and the applied voltage varies. Of course, it is possible that the applied voltage is given and the uniform hydrostatic pressure varies, as will be seen in section 6 below.

4.1. Solution to Normal Mode

For this mode, the boundary conditions at the center are

$$w(0)=w_0,\frac{dw(0)}{dr}=\frac{d^3w(0)}{dr^3}=0,\frac{d^2w(0)}{dr^2}=w_0'' \tag{14}$$

where the deflection at the center w_0 is given; the second derivative at the center w_0'' and the applied voltage U are unknown (before pull-in phenomenon, it is possible that the applied voltage is given and the deflection at the center w_0 and the second derivative at the center w_0'' are unknown). These two unknowns can be obtained with a two-fold method of bisection based on the shooting method from the conditions that both the deflection and the slope at the clamped edge of the circular micro plate are zero (the detail can be seen in [9], although the model in [9] is for a direct metal-metal contact type MEMS switch and the differential governing equation is also different). Obtaining the second derivative at the center w_0'' and the applied voltage U, one can numerically calculate the deflection $w(r)$ and its first three derivatives at any point with some numerical technique easily from equation (8). One can also calculate the volume change percentage V_P [24] between the circular flexible plate and the dielectric layer or the ratio of the capacitance C_R [25] between two electrodes numerically as follows

$$V_P=\frac{\int_0^a 2\pi w(r)rdr}{\pi a^2 g}=\frac{2\int_0^a w(r)rdr}{a^2 g} \tag{15}$$

$$C_R = \frac{\varepsilon_0 \int_0^a \frac{2\pi r}{G - w(r)} dr}{\left(\frac{\varepsilon_0 \pi a^2}{G}\right)} = \frac{2G \int_0^a \frac{r}{G - w(r)} dr}{a^2} \quad (16)$$

Incorporating the above numerical solution to the applied voltage with some constrained optimization method, such as Powell's method [26], the pull-in voltage and the corresponding pull-in position can automatically be obtained on a computer with less manual intervention.

4.2. Solution to Transition Mode

For this mode, the boundary conditions at the center are

$$w(0) = g, \frac{dw(0)}{dr} = \frac{d^3 w(0)}{dr^3} = 0, \frac{d^2 w(0)}{dr^2} = w_0'' \quad (17)$$

At this mode, the differential governing equation is (10), the second derivative at the center w_0'' is given, and the applied voltage U and the force $q_1(r)$ distributed over the area of radius δ are unknown. In the paper, the force $q_1(r)$ is considered the distribution of pressure over the contact surface between the two bodies(one is the micro circular plate, and another is the substrate with the dielectric layer as shown in Fig. 1) and assumed, using the contact theory [27], as follows

$$q_1(r) = \frac{3P}{2\pi\delta^3}\sqrt{\delta^2 - r^2} \quad (18)$$

or, for simplicity, the distribution of pressure over the contact surface is assumed as

$$q_1(r) = \frac{P}{\pi\delta^2} \quad (19)$$

where P is the total force over the contact surface, and δ is given in practice.

At this mode, the applied voltage U and the total force P are unknown. Similar to the normal mode, these two unknowns can also be obtained with the two-fold method of bisection from the conditions that both the deflection and the slope at the clamped edge of the micro circular plate are zero.

4.3. Solution to Touch Mode

Because of $w(r) \equiv g$ in the range $[0, \Delta]$ at this mode, we should only calculate the deformations in the range $[\Delta, a]$, and boundary conditions at $r = \Delta$ are

$$w(\Delta) = g, \frac{dw(\Delta)}{dr} = \frac{d^2 w(\Delta)}{dr^2} = 0, \frac{d^3 w(\Delta)}{dr^3} = w_\Delta''' \quad (20)$$

The differential governing equation without singularity is

$$D\left(\frac{d^4 w}{dr^4} + \frac{2}{r}\frac{d^3 w}{dr^3} - \frac{1}{r^2}\frac{d^2 w}{dr^2} + \frac{1}{r^3}\frac{dw}{dr}\right) - \frac{\pi t}{r}\frac{d}{dr}\left(r\frac{dw}{dr}\right) = q(r, w, U, q_0) \qquad \Delta \le r \le a \quad (21)$$

At this mode, the applied voltage U and the third derivative w_Δ''' are unknown with Δ being given. Similar to the first two modes, these two unknowns can be obtained with the two-fold method of bisection from the conditions that both the deflection and the slope at the clamped edge of the circular micro plate are zero.

5. Examples

5.1. Entire Deformation Analysis of a Micro Circular Plate

In this example, an entire analysis for the three different modes will be performed. The material and geometrical parameters in the example are listed in Table 1. All parameters except the relative permittivity and the thickness of the dielectric layer come from [13], in which these two parameters are useless because the normal mode before the pull-in phenomenon was only analyzed.

Table 1. Material and geometrical parameters.

Symbol	Quantity	Value
E	Modulus of elasticity	169 GPa
μ	Poisson's ratio	0.3
ε_0	Vacuum permittivity	8.854×10^{-12} F·m^{-1}
ε_1	Relative permittivity of the dielectric layer	8.36
ε_r	Relative permittivity of air	1.0
a	Radius of the circular plate	250 μm
t	Thickness of the circular plate	20 μm
t_1	Thickness of the dielectric layer*	1.0 μm
g	Initial gap	1.0 μm
τ	residual biaxial plane stress	0
q_0	Hydrostatic pressure	0

*Note: the breakdown voltage is in a range from 6 MV/cm to 12 MV/cm from an inspection to the breakdown histogram for silicon-nitride film [28].

Fig. 4 shows the applied voltage versus the center deflection of the micro circular plate at the normal mode. The second derivative at the center of the micro circular plate versus the center deflection of the micro circular plate is shown in Fig. 5. The

corresponding figures to demonstrate the volume change percentage or the ratio of the capacitance versus the center deflection of the micro circular plate at the normal mode are presented in Fig. 6 and Fig. 7. The pull-in voltage U_{PI} is about 373.62 V, and the related center deflection, the volume change percentage and the ratio of the capacitance are about 0.52 μm, 16.5 %, and 1.21 respectively. The applied voltage and the minimum second derivative at the center w_0'' are about 225.37 V and -1.0017×10^{-4} at the end of the mode, respectively.

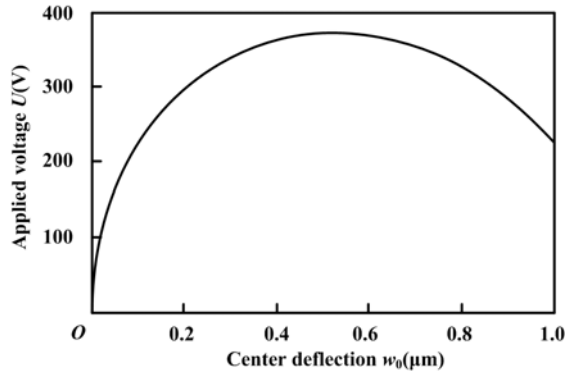

Fig. 4. Applied voltage versus center deflection.

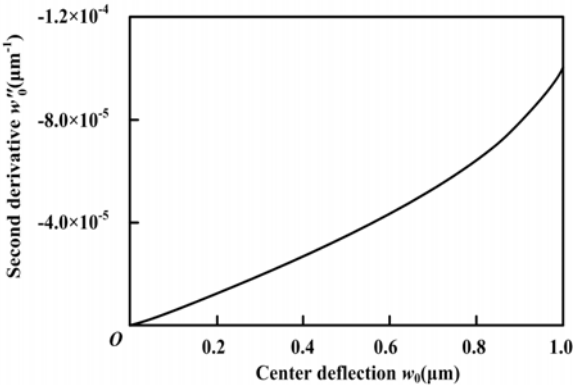

Fig. 5. Second derivative w_0'' versus center deflection.

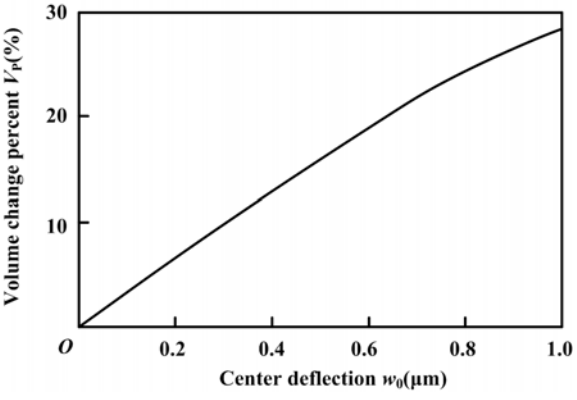

Fig. 6. Volume change percent versus center deflection.

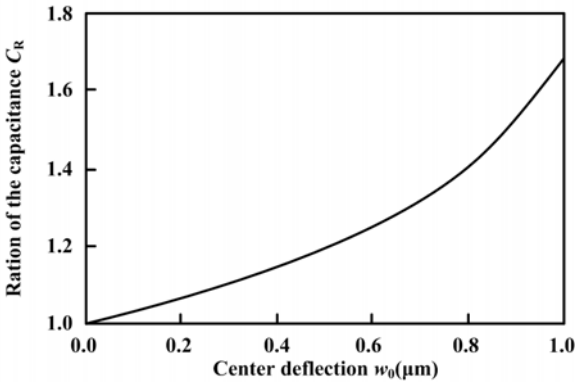

Fig. 7. Ratio of the capacitance versus center deflection.

At the transition mode, a numerical analysis of the solid circular plate is complicated by the fact that a concentrated reaction acts at the center of the circular plate. In this work, the concentrated force is replaced by a force distributed over a small circular area as shown in equation (18) or in equation (19) with a radius δ . Some computed results for the different radiuses δ are listed in Table 2 and Table 3 for two different distributions of pressure.

Table 2. Some applied voltages and the total forces obtained with the second derivative $w_0'' = 0.0$ and some different radiuses in Eqn. (18).

Radius δ (μm)	Applied voltage U (V)	Total force P (μN)
6.5	258.83	6.8349×10^4
5.0	256.56	6.1409×10^4
3.0	252.96	5.1216×10^4
1.0	247.46	3.7682×10^4
1.0×10^{-2}	237.27	1.7842×10^4
1.0×10^{-4}	233.49	1.1684×10^4
1.0×10^{-6}	231.53	8.6120×10^4
1.0×10^{-8}	230.34	6.7086×10^3

Table 3. Some applied voltages and the total forces obtained with the second derivative $w_0'' = 0.0$ and some different radiuses in Eqn.(19).

Radius δ (μm)	Applied voltage U (V)	Total force P (μN)
6.5	260.14	7.2728×10^4
5.0	257.70	6.4947×10^4
3.0	253.85	5.3672×10^4
1.0	248.04	3.9002×10^4
1.0×10^{-2}	237.45	1.8132×10^4
1.0×10^{-4}	233.57	1.1785×10^4
1.0×10^{-6}	231.56	1.0277×10^4
1.0×10^{-8}	230.38	6.0441×10^3

It can be seen from Table 2 that there is few change in the applied voltage for both two different distributions of pressure when $\delta < 1.0 \times 10^{-4}$, although the total forces quite differ for different

radiuses or different distributions. We will not concern ourselves unduly with the effect of the radius δ , because the transition mode is only a temporary, uncontrollable state, as it is expressed by the term "transition mode". $\delta = 1.0 \times 10^{-6}\ \mu m$, which is much smaller than $\delta = 0.325t = 6.5\ \mu m$ suggested in [29] and can at least give the first two correct digitals of the applied voltage (the relative error is less than 1.0 %), and the distribution of pressure in equation (18) are used to obtain the below results.

Fig. 8 shows the applied voltage versus the second derivative at the center of the micro circular plate at the transition mode. Fig. 9 shows the total force over the circular area of radius $\delta = 1.0 \times 10^{-6}\ \mu m$ versus the second derivative at the center.

The corresponding figures to demonstrate the volume change percentage or the ratio of the capacitance versus the second derivative at the center are presented in Fig. 10 and Fig. 11. The applied voltage is about 231.53 V at the end of the mode.

Fig. 12 shows the applied voltage versus the contact radius at the touch mode. Because the change range of the third derivative at $r = \Delta$ during the touch mode is too large to observe its behavior clearly in one figure, three figures over three different ranges for contact radius (from 0.0001 μm to 0.01 μm, from 0.01 μm to 1.0 μm, and from 1.0 μm to 100 μm) are used to describe its behavior shown in Fig. 13(a)-Fig. 13(c). The corresponding figures to demonstrate the volume change percentage or the ratio of the capacitance versus contact radius at the touch mode are presented in Fig. 14 and Fig. 15.

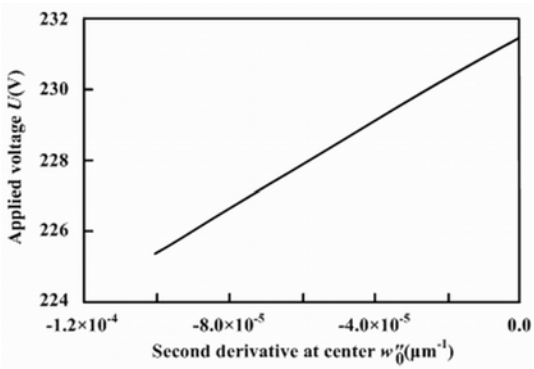

Fig. 8. Applied voltage versus second derivative.

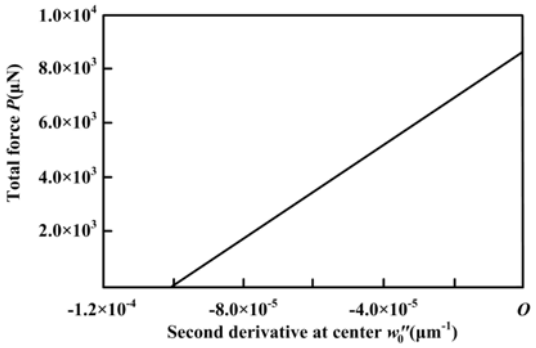

Fig. 9. Total force versus second derivative.

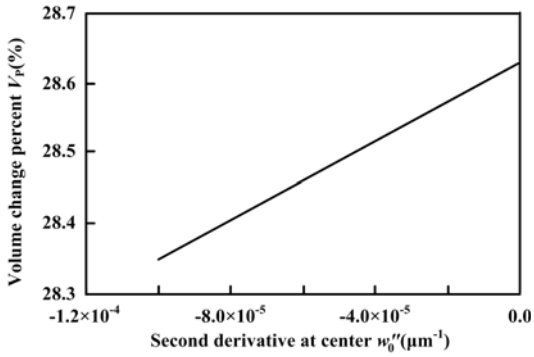

Fig. 10. Volume change percent versus second derivative.

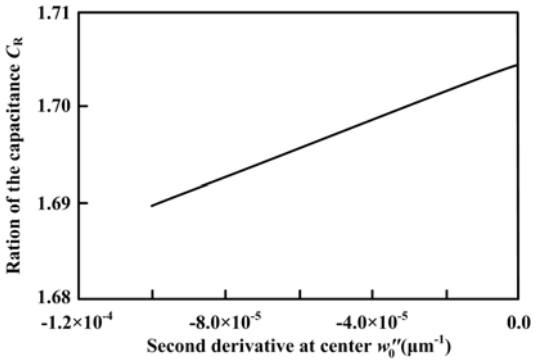

Fig. 11. Ratio of the capacitance versus second derivative.

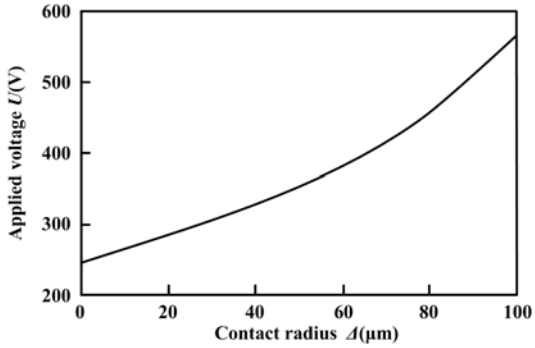

Fig. 12. Applied voltage versus contact radius.

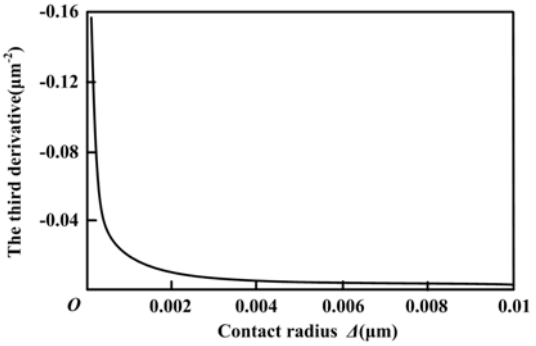

Fig. 13 (a). The third derivative versus contact radius.

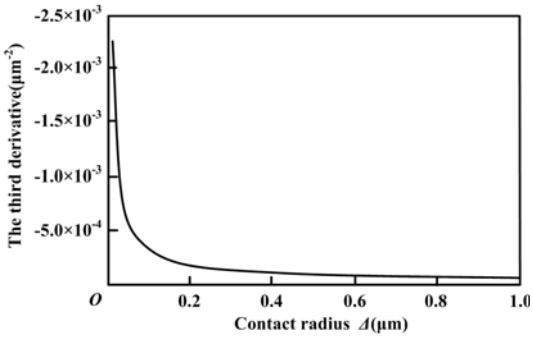

Fig. 13 (b). The third derivative versus contact radius.

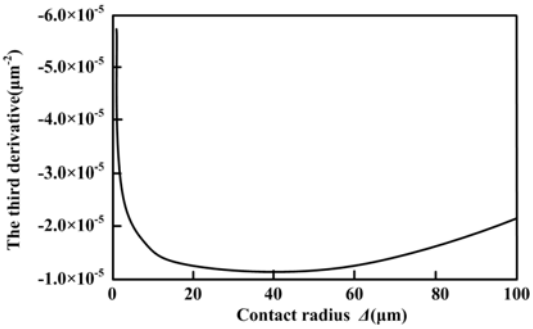

Fig. 13 (c). The third derivative versus contact radius.

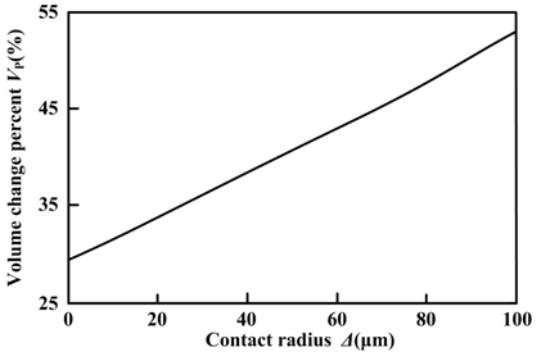

Fig. 14. Volume change percent versus contact radius.

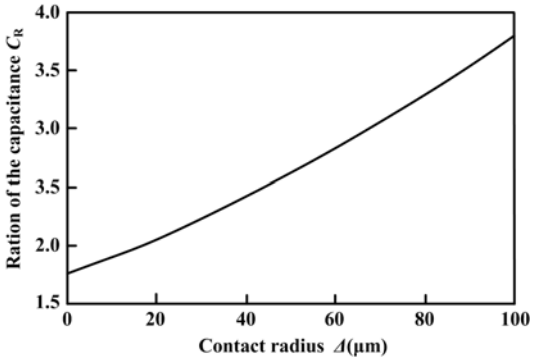

Fig. 15. Ratio of the capacitance versus contact radius.

5.2. Effect of Some Parameters on the Pull-in Voltage

In this example, the effect of some geometry dimensions, the radius and the thickness of the micro circular plate, the thickness of the dielectric layer, the initial gap, the uniform hydrostatic pressure, and the residual stress on the pull-in voltage will be analyzed. Note please that in the example, all parameters are the same as the Table 1 except for the parameter under discussion.

The relation between the radius of the plate and the pull-in voltage is shown in Fig. 16. The relation between the thickness of the plate and the pull-in voltage is shown in Fig. 17. The relation between the thickness of the dielectric layer and the pull-in voltage is shown in Fig. 18. The relation between the initial gap between the plate and the dielectric and the pull-in voltage is shown in Fig. 19. The relation between the uniform hydrostatic pressure and the pull-in voltage is shown in Fig. 20. The relation between the residual stress and the pull-in voltage is shown in Fig. 21.

Figs. 16 - 21 show how the pull-in voltage varies with a parameter.

6. Comparison with Some Other Results

Some obtained pull-in voltages without the dielectric layer for only electrostatic actuation are compared with some existing results as presented in Table 4-6.

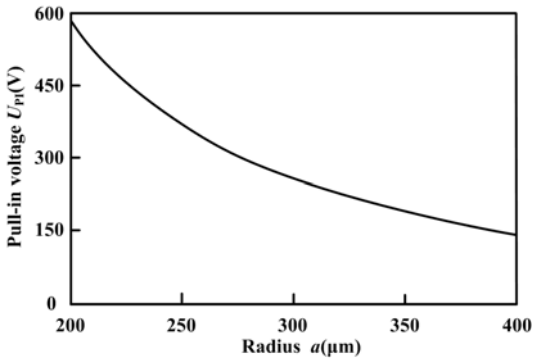

Fig. 16. Radius of the plate versus pull-in voltage.

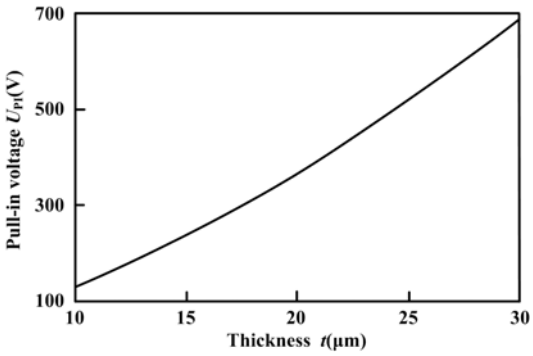

Fig. 17. Thickness of the plate versus pull-in voltage.

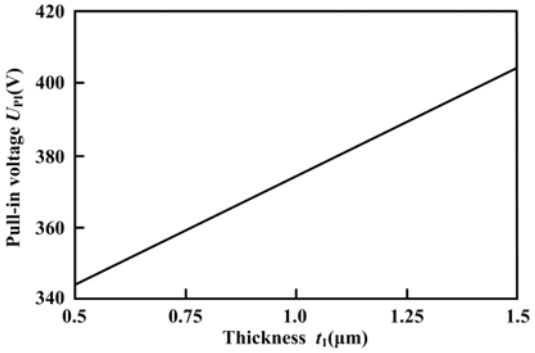

Fig. 18. Thickness the dielectric layer versus pull-in voltage.

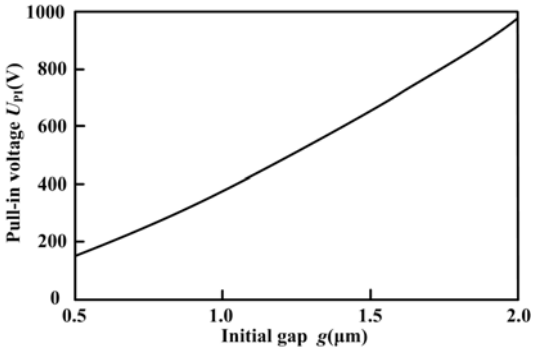

Fig. 19. Initial gap versus pull-in voltage.

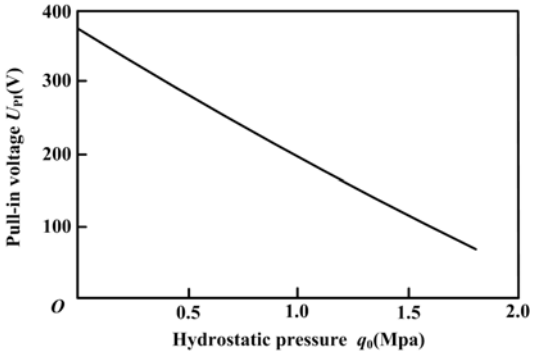

Fig. 20. Uniform hydrostatic pressure versus pull-in voltage.

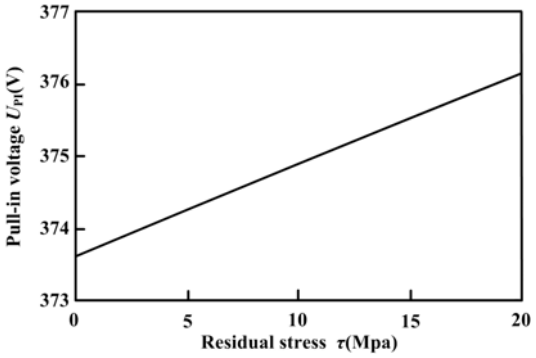

Fig. 21. Residual stress versus pull-in voltage.

Table 4. Pull-in voltages obtained with two different methods for some radiuses of the plate.

Radius a(μm)	Pull-in voltage U_{PI}(V)in [12]	Pull-in voltage U_{PI}(V) in this paper	Relative error*(%)
240	342.34	342.20	-0.041
250	315.51	315.34	-0.054
260	291.70	291.58	-0.041

*The relative error is calculated with (result in this paper-result in reference)×100/result in this paper.

Table 5. Pull-in voltages obtained with two different methods for some thicknesses of the plate.

Thickness t(μm)	Pull-in voltage U_{PI}(V)in [12]	Pull-in voltage U_{PI}(V) in this paper	Relative error (%)
19	292.14	292.03	-0.038
20	315.51	315.34	-0.054
21	339.46	339.32	-0.041

Table 6. Pull-in voltages obtained with two different methods for some initial gap.

Initial gap g (μm)	Pull-in voltage U_{PI}(V)in [12]	Pull-in voltage U_{PI}(V) in this paper	Relative error (%)
0.9	269.39	269.26	-0.048
1.0	315.51	315.34	-0.054
1.1	363.99	363.82	-0.047

Some deflections at the center of the plate for several different hydrostatic pressures for a constant applied voltage 100 V are listed in Table 7, and some deflections at the center of the plate for several different applied voltages for a constant hydrostatic pressure 200 kPa are listed in Table 8. The deflections listed in Table 7 and Table 8 are all values before pull-in phenomenon.

Table 7. Deflections at the center obtained with two different methods for U=100 V.

Hydrostatic pressure q_0 (kPa)	Deflection w_0(μm) in [13]	Deflection w_0(μm) in this paper	Relative error (%)
0	0.02367	0.02248	-5.29
200	0.12862	0.12444	-3.36
700	0.39804	0.38535	-3.29
1200	0.71870	0.68017	-5.66

Table 8. Deflections at the center obtained with two different methods for q_0=200 kPa.

Applied voltage U(V)	Deflection w_0(μm) in [13]	Deflection w_0(μm) in this paper	Relative error (%)
0*	0.10184	0.09858	-3.31
100	0.12862	0.12444	-3.36
200	0.22639	0.21752	-4.08
280	0.64154	0.47685	-34.54

* Note: the theoretical deflection at the center [20] for the applied voltage $U = 0$ is $w_0 = \frac{q_0 a^4}{64D} = 0.098595$ μm .

It can be seen from Table 4-Table 8 that good agreement except for one case of the applied voltage 280 V in Table 8 has been achieved.

Another comparison is also made. The pull-in voltages obtained in this paper and in [17] are 19.2194 V and 20.1792 V respectively with parameter values of $a = 250\ \mu m$, $t = 3.01\ \mu m$, $g = 1.014\ \mu m$, $E = 150.6\ Gpa$, $\nu = 0.0435$, and $\tau = 7.8\ Mpa$. The relative error is -4.99 %.

7. Conclusions

A distributed model with three possible static modes was presented to investigate the behavior of the plate subjected to electrostatic force and uniform hydrostatic pressure both before pull in and beyond pull in. The differential governing equation of the micro circular plate specifically used for numerical solution of the three modes without singularity was presented based on the classical thin plate theory, Taylor's series expansion and Saint-Venant's principle.

The numerical solution to the differential governing equation for the different mode was mainly attributed to solve for one unknown boundary condition and the applied voltage, which could be obtained by using a two-fold method of bisection based on the shooting method. Because the deflection at the center was given, which avoided the numerical interpenetration between the circular plate and the dielectric layer due to the computation error, and solution to the differential governing equation could be directly obtained without accumulated error for both before pull-in and after pull-in phenomenon, some constrained optimization method can be incorporated to the solution to obtain pull-in voltage automatically on a computer with less manual intervention.

The control to the error in this method is very simple, and the method can be carried to any degree of accuracy desired with little try at the expense of time and computer costs.

In examples, the entire mechanical behavior of the circular plate over the operational voltage ranges was investigated and the effects of different parameters, such as radius and thickness of the plate, thickness of the dielectric layer, uniform hydrostatic pressure, uniform residual stress and initial gap on pull-in voltage were studied. From comparison with some other obtained results, good agreement is achieved.

References

[1]. H. C. Nathanson, W. E. Newell, R. A. Wickstrom, J. R. Davis, The resonant gate transistor, *IEEE Transaction on Electron Devices*, Vol. 14, 1967, pp. 117–133.

[2]. G. I. Taylor, The coalescence of closely spaced drops when they are at different electric potentials, *Proceedings of Royal Society A*, Vol. 306, 1968, pp. 423–434.

[3]. H. A. C. Tilmans, Equivalent circuit representation of electromechanical transducers: I. lumped-parameter systems, *Journal of Micromechanics and Microengineering*, Vol. 6, 1996, pp. 157–176.

[4]. J. M. Huang, K. M. Liew, C. H. Wong, S. Rajendran, M. J. Tan, A. Q. Liu, Mechanical design and optimization of capacitive micromachined switch, *Sensors and Actuators A*, Vol. 93, 2001, pp. 273–285.

[5]. V. T. Srikar, S. M. Spearing, Materials selection for microfabricated electrostatic actuators, *Sensors and Actuators A*, Vol. 102, 2003, pp. 279–285.

[6]. S. Gorthi, A. Mohanty, A. Chatterjee, Cantilever beam electrostatic MEMS actuators beyond pull-in, *Journal of Micromechanics and Microengineering*, Vol. 16, 2006, pp. 1800–1810.

[7]. H. Sadeghian, G. Rezazadeh, E. Abbaspour, A. Tahmasebi, I. Hosainzadeh, The effect of residual stress on pull-in voltage of fixed-fixed end type MEM switches with variative electrostatic area, in *Proceedings of the 1st IEEE International Conference on 'Nano/Micro Engineered and Molecular Systems'*, Zhuhai, China, 18-21 January, 2006, pp. 1117–1120.

[8]. P. M. Zavracky, S. Majumder, N. E. McGruer, Micromechanical switches fabricated using nickel surface micromachining, *Journal of*

Microelectromechanical System, Vol. 6, Issue 1, 1997, pp. 3–9.
[9]. T. J. Cao, F. Ding, Static Analysis Model of Micro-machined Switch Consisting of Clamped-Clamped Beam (in Chinese), *Engineering Mechanics*, Vol. 23, Issue 9, 2006, pp. 42-47, 54.
[10]. E. S. Hung, S. D. Senturia, Generating efficient dynamical models for microelectromechanical systems from a few finite-element simulations runs, *Journal of Microelectromechanical System*, Vol. 8, Issue 3, 1999, pp. 280–289.
[11]. E. K. Chan, K. Garikipati, R. W. Dutton, Characterization of contact electromechanics through capacitance-voltage measurements and simulations, *Journal of Microelectromechanical System*, Vol. 8, Issue 2, 1999, pp. 208–217.
[12]. P. Soleymani, H. Sadeghian, A. Tahmasebi, G. Rezazadeh, Pull-in instability investigation of circular micro pump subjected to nonlinear electrostatic force, *Sensors & Transducers*, Vol. 69, Issue 7, July 2006, pp. 622–628.
[13]. Nabian, G. Rezazadeh, M. Haddad-Derafshi, A. Tahmasebi, Mechanical behavior of a circular micro plate subjected to uniform hydrostatic and non-uniform electrostatic pressure, *Microsystem Technologies*, Vol. 14, 2008, pp. 235–240.
[14]. M. Rahman, S. Chowdhury, A Highly Accurate Method to Calculate Capacitance of MEMS Sensors with Circular Membranes, in *Proceedings of the IEEE International Conference on Electro/Information Technology*, Windsor, Canada, 7-9, June, 2009, pp. 178–181.
[15]. C. C. Chen, Y. T. Cheng, Physical Analysis of a Biomimetic Microphone With a Central-Supported (C-S) Circular Diaphragm for Sound Source Localization, *IEEE Sensors Journal*, Vol. 12, Issue 5, 2012, pp. 1504–1512.
[16]. P. Li, Y. M. Fang, R. F. Hu, Thermoelastic damping in rectangular and circular microplate resonators, *Journal of Sound and Vibration*, Vol. 331, 2012, pp. 721–733.
[17]. L. D. Liao, P. C. P. Chao, C. W. Huang, C. W. Chiu, dc dynamic and static pull-in predictions and analysis for electrostatically actuated clamped circular micro-plates based on a continuous model, *Journal of Micromechanics and Microengineering*, Vol. 20, 2010, pp. 1–15.
[18]. Q. Wang, W. H. Ko, Modeling of touch mode capacitive sensors and diaphragms, *Sensors and Actuators*, Vol. 75, 1999, pp. 230–241.
[19]. G. Fragiacomo, T. Ansbæk, T. Pedersena, O. Hansen, E. V. Thomsena, Analysis of small deflection touch mode behavior in capacitive pressure sensors. *Sensors and Actuators A: Physical*, Vol. 161, 2010, pp. 114–119.
[20]. S. Timoshenko, S. Woinowsky-Krieger, Theory of plates and shells (2nd Edition), *McGraw-Hill Book Company,* 1959.
[21]. M. H. Sadd, Elasticity: Theory, Applications, and Numerics, *Elsevier Butterworth–Heinemann*, 2005.
[22]. G. M, Wen, H. Ko, Modeling of circular diaphragm and spreadsheet solution programming for touch mode capacitive sensors, *Sensors and Actuators*, Vol. 75, 1999, pp. 45–52.
[23]. David Kincaid, Ward Cheney, Numerical analysis: mathematics of scientific computing (3rd Edition), *China Machine Press,* 2003.
[24]. F. Amirouche, Y. Zhou, T. Johnson, Current micropump technologies and their biomedical applications, *Microsystem Technologies,* Vol. 15, 2009, pp. 647–666.
[25]. Z. J. Yao, S. Chen, S. Eshelman, D. Denniston, C. Goldsmith, Micromachined low-loss microwave switches, *Microelectromechanical Systems*, Vol. 8, Issue 2, 1999, pp. 129–134.
[26]. D. G. Liu, Collection of algorithms in Fortran language, part 2 (in Chinese), *National Defence Industry Press,* 1983.
[27]. S. Timoshenko, J. N. Goodier, Theory of Elasticity (3rd Edition), *Tsinghua University Press*, 2004.
[28]. S. H. Lee, M. G. So, Characteristics of thin nitrided oxides prepared by an in-situ process, *Journal of Materials Science,* Vol. 28, 1993, pp. 6645-6649.
[29]. W. C. Young, R. G. Budynas, Roark's formulas for stress and strain (7th Edition), *Tsinghua University Press,* 2003.